A radial mode ultrasonic horn for the inactivation of *Escherichia coli* K12

G. Hunter, M. Lucas*, I. Watson, R. Parton#
Department of Mechanical Engineering, University Of Glasgow, Glasgow G12 8QQ, UK
Division of Infection and Immunity, University Of Glasgow, Glasgow G12 8QQ, UK

Abstract
Tuned cylindrical radial mode ultrasonic horns offer advantages over ultrasonic probes in the design of flow-through devices for bacterial inactivation. This study presents a comparison of the effectiveness of a radial horn and probe in the inactivation of *E. coli* K12. The radial horn is designed using finite element analysis and the predicted modal parameters are validated using experimental modal analysis. A validated finite element model of the probe is also presented. Visual studies of the cavitation fields produced by the radial horn and probe are carried out using luminol and also backlighting to demonstrate the advantages of radial horns in producing a more focused cavitation field with widely dispersed streamers. Microbiological studies show that, for the same power density, better inactivation of *E. coli* K12 is achieved using the radial horn and, also, the radial horn offers greater achievable power density resulting in further improvements in bacterial inactivation. The radial horn is shown to be more effective than the probe device and offers opportunities to design in-line flow-through devices for processing applications.

Keywords: Cavitation, Bacterial inactivation, Radial horn, Ultrasonics, *E. coli*

* Corresponding author.
Department of Mechanical Engineering, University of Glasgow, Glasgow, G12 8QQ, Scotland, UK
Tel: +44 (0)141 330 4323
Fax: +44 (0)141 330 4343
E-mail address: m.lucas@mech.gla.ac.uk (M. Lucas)

1. Introduction

The ability of ultrasound to inactivate bacterial cells has been studied for many years but early research indicated that it was not a cost-effective method [1]. However, with the development of more powerful transducers there has been renewed interest in this area. Alternative methods for bacterial inactivation, for example in liquid food products and in wastewater treatment, are being sought to improve the quality of the end product. Inactivation methods in the food processing industry normally rely on heat, as in pasteurisation, while the water industry largely relies on chemicals to inactivate cells. These methods work well, but exposure to high temperatures and chemicals, particularly chlorine, may cause detrimental effects to the taste and quality of the end product. The use of chemicals is also highly regulated, and bacterial cells are becoming more resistant to chemical treatments [2]. Furthermore, these treatments may not be effective under certain conditions, such as high initial cell counts [3,4] and consequently there is a need to develop new or emerging technologies that satisfy sterility requirements. Ultrasonic processing is an effective way of achieving non-thermal inactivation, allowing treatment of heat-sensitive material.

The mechanism of ultrasonic bacterial inactivation is through the interaction of cavitation bubbles and the microorganism. Cavitation bubbles are formed and grow when a liquid is put in a significant state of tension. Liquids, though unable to support shear stresses, can support compressive stresses and, for short periods, tensile stresses. When a pressure wave is applied to a liquid it undergoes a compression and rarefaction cycle and, during the rarefaction half-cycle, the pressure in the liquid becomes negative. If the magnitude of this negative pressure is sufficiently high, voids or bubbles are created [5]. In theory [6], it would take a negative pressure in excess of 100 MPa to overcome the attractive molecular forces in water. In practice, however, the maximum achievable negative pressure is in the order of 10 MPa [7] using ultrafiltration and purification techniques. Normal household tap water has measured threshold values between 0.01-0.5 MPa [8]. This is thought to be due to microscopic bubbles dissolved in the fluid or microscopic particles, such as minerals, acting as nucleation sites [9].

During transient cavitation, bubbles expand rapidly under tension and collapse violently as the pressure wave moves from tensile to compressive. When the bubble collapses, a high local temperature is achieved, possibly in the order of 5000 K [10]. This temperature rise has largely been rejected as the main cause of bacterial inactivation due to its very localised nature, as only a small number of bacteria would be subjected to these temperatures. Another mechanism which has been widely attributed to the inactivation of bacteria during cavitation is the pressure shock wave of up to 50 MPa which is created when a cavitation bubble collapses. Although bacteria are known to withstand large static pressures they seem to be susceptible to rapidly alternating pressures [11].

Traditionally, the device used for cell disruption has been the ultrasonic probe. This device works at a fixed ultrasonic frequency, normally between 20 and 50 kHz and is designed to be resonant in a longitudinal mode of vibration. The probe is a tuned ultrasonic horn, shaped to provide a relatively large vibration amplitude gain. A typical vibration amplitude at the tip is about 100 μm with an output from the transducer of about 10 μm.

Ultrasonic inactivation alone is too slow to be useful in most flow processes [11]. Consequently, there have been relatively few studies researching the use of ultrasonics as a bactericidal technology in flow-through systems [1,12,13,14]. These studies have concentrated on adapting a fluid system to incorporate an ultrasonic probe with the flow rates being very low (<0.5 litres/minute). The ultrasonic probe may not be ideal for flow-

through devices, even for very low flow-rates, as the cavitation field is concentrated in a cone shape in front of the tip of the probe and not distributed across the flow. This study therefore investigates the use of a radial mode ultrasonic horn, which could be more readily adapted as an in-line flow-through bacterial inactivation device. The performance of the radial horn was compared with an ultrasonic probe in order to assess its effectiveness in terms of the bacterial inactivation rate for the same power density.

2. The Ultrasonic Devices

2.1 Radial ultrasonic horn

A radial ultrasonic horn was designed and tuned using finite element analysis (FEA). The cylindrical horn was tuned to its fundamental radial mode, a mode of vibration which involves a radial stretch then contraction of the whole cylinder through its vibration cycle and referred to as the R0 mode, at the operating frequency of 20 kHz. The radial horn is shown in Figure 1 and consists of a thick cylinder of mean radius 47 mm, which results in tuning to the R0 mode at 20 kHz. An outer and inner radius can then be selected to provide the desired volume of the fluid cavity. The attached thin cylinders are subsequently positioned and tuned at 20 kHz such that they provide nodal structural mounting flanges and anti-nodal attachments to the thick cylinder. The horn was manufactured from aluminium having a Young's modulus of 71 GN/m^2, density 2700 kg/m^3 and Poisson's ratio of 0.33. The horn and tuned connecting flanges provide a profile adaptable to a flow-through process and the radial mode is used in order to focus the ultrasonic energy at the centre of the horn cavity [9,15]. The aim is to produce an area of low pressure where cavitation can occur in the fluid away from the vibrating face at the inner diameter of the cylinder. Also, by focussing the ultrasonic energy, it is possible to achieve a cavitation cloud at significantly lower ultrasonic amplitudes than is necessary with probe devices.

A finite element (FE) model was created using ABAQUS (Abaqus Inc.) as the pre-processor, solver and post-processor. The model used 20 node quadratic solid brick elements throughout and the mode shapes and frequencies were determined using the Lanczos solver. The model was meshed using 1443 elements, to ensure a converged solution, as shown in Figure 2.

In order to confirm the predicted modal parameters of frequencies and mode shapes, an experimental modal analysis (EMA) was carried out using a 3D Laser Doppler Vibrometer (LDV) connected to LMS Cada-X data acquisition and post-processing software (LMS Inc.). The 3D LDV (Polytec) allows non-contact vibration velocity measurements from a grid of measurement points on the target surface. One out-of-plane and two in-plane surface vibration velocity components are acquired using the 3D LDV. The EMA was carried out for a frequency range of 10-30 kHz, chosen in order to extract the modes in the frequency range close to and centred on the tuned frequency of 20 kHz. Also, the ultrasonic transducer used can easily excite this frequency range whilst maintaining good signal coherence. By monitoring the random excitation signal and the three components of each target point vibration velocity, a series of frequency response functions (FRFs) were acquired over the surface of the horn.

Figure 3 shows a comparison of the modes and frequencies from the FEA and EMA. The radial modes excited in the frequency range are shown in the figure, with only the outer diameter measurement points shown for the EMA for clarity. It is seen that there is good agreement between the EMA and FEA in terms of mode shapes and modal frequencies, with less than 0.5 % difference between predicted and measured modal frequencies for the three modes in the range. As is typical of thick cylinders, the fundamental, first and third radial modes, R0, R1 and R3 respectively, are grouped within a relatively small frequency

band [16] and separation of these modal frequencies is vital to the successful design of such horns. Previous studies suggest that a frequency separation of the tuned mode from other non-tuned modes of 1200 Hz is necessary at 20 kHz to ensure there is no significant modal coupling [17]. In this case, the tuned modal frequency satisfies this frequency separation criteria and, consequently, the horn can excite a pure R0 mode with high vibration amplitude uniformity at its inner diameter output surface.

The sum of all the measured FRF's between 16 kHz and 25 kHz is shown in Figure 4(a). It can be observed that there are three distinct modes in this range, the R1, R0 and R3 modes. There also appears to be a small fourth response peak embedded in the response of the third mode at approximately 22 kHz and this peak has been confirmed to be the dual R3 mode caused by minor asymmetries in the shape of the radial horn [18].

2.2 Ultrasonic probe

A similar experimental analysis was performed for the probe device. The probe device was a Jencons VCX 400 with a standard 13 mm horn attached to the transducer, with a titanium tip to minimise damage caused through cavitation. A finite element model of the probe was constructed in ABAQUS and the modal frequencies and mode shapes were extracted. The model used 1894 elements with the same 20 node quadratic brick elements as were used for the radial horn. It can be seen from Figure 4(b) and Figure 5 that the probe resonates in a longitudinal mode at 20026 Hz with the third bending and second torsional modes occurring at 21794 Hz and 23804 Hz respectively. The differences between the EMA and FEA estimated modal frequencies were within 1.6 %, providing good correlation.

Both ultrasonic horns have been shown to operate in their tuned mode of vibration without significant coupling of non-tuned modes and, in particular, the radial horn designed for this study can provide a uniform vibration amplitude, at its inner diameter output surface, to the fluid in the cylinder cavity.

3. Methods and Materials

3.1 Comparison criteria

In defining criteria for comparing the radial horn and probe, it was recognised that the two devices have different ideal setups. Thus it was proposed that the devices should be compared in a manner consistent with other published studies [19,20,21]. The power input of both devices was measured, where the probe device was connected to a generator that displayed the power input in Watts, and for the radial horn the power input was estimated by a calorific method [22]. Using this method, it was assumed that all the ultrasonic energy was eventually converted into heat, thus producing a rise in the bulk temperature of the horn and contained fluid. This rise in temperature can therefore be related to the energy input using equation (1).

$$E = mC_p\Delta T \quad (1)$$

where m is the mass being sonicated, C_p the specific heat capacity (0.9 kJ/kgK and 4.186 kJ/kgK for aluminium and water respectively) and ΔT the temperature rise in Kelvin, measured using a thermometer. The power input, P, can then be calculated from equation (2).

$$E = Pt \quad (2)$$

where t is the time taken to achieve the temperature rise in seconds.

In previous studies, two main criteria have been used to compare ultrasonic devices; ultrasonic intensity and power density. Ultrasonic intensity is defined in units of Watts per square centimetre (W/cm^2) of horn working surface [19,20] and power density as Watts per

cubic centimetre (W/cm^3) of the sonicated volume [20]. In this study, both are presented but only power density can be used for comparative purposes since the output surface area of the radial horn is over 30 times greater than that of the probe. For consistency, the power density measurements for the probe horn were carried out in the same sonicated volume as the radial horn.

3.2 Cavitation field visualisation

The cavitation field was visualised using two methods; a chemical method and the other based on the refraction of light caused by cavitation bubble clouds. It is known that cavitation can cause sonochemiluminescence (SCL) through chemical reactions involving luminol (3-aminophthalhydrazide, 97%) and hydrogen peroxide (H_2O_2) [23,24]. The cavitational collapse of bubbles causes the release of $HO^{\cdot}$ free radicals which react with the luminol solution. These free radicals are also known to have a bactericidal effect [25]. Hydrogen peroxide is used as an oxidiser and enhances this reaction. Two solutions were made. The first consisted of 0.1 g of luminol ($C_8H_7N_3O_2$), 0.5 g of ammonium carbonate ($(NH_4)_2CO_3$), 4 g of sodium carbonate (Na_2CO_3) and 24 g of sodium bicarbonate ($NaHCO_3$) dissolved in 1 litre of distilled water (H_2O). The second consisted of 25 ml of 6 % hydrogen peroxide (H_2O_2) diluted in 1 litre of distilled water. The two solutions were then mixed in equal quantities to achieve the final solution. It is known that the intensity of cavitation induced sonochemiluminescence is dependent on the *p*H of the solution [11], with the greatest intensity observed at a *p*H of 12. Two *p*H levels were used in these tests; *p*H 9.5 and *p*H 12. The *p*H was altered by adding Sodium Hydroxide (NaOH) to the working solution. This provided an intensity that could easily be captured by a digital camera on a long exposure setting in a dark room. All solutions were used within 12 hours of preparation. The solution was poured into the cylindrical horn cavity and photographs of the luminescence were taken using a digital camera (Canon Eos 350D). The probe horn was partially immersed in a clear beaker filled with luminol solution and photographs were taken using the same settings as those for the radial horn.

3.3 Bacterial inactivation experiments

For the bacterial inactivation experiments an aseptic technique was used throughout. The radial horn was mounted on an aluminium base with the fluid sealing provided through a rubber gasket. In order to observe the bactericidal efficacy of the horn, rather than the combination of the horn and its mounting structure, it was necessary to have as little fluid as possible in the tuned mounting section. This was achieved by inserting a loose fitting plastic cylinder into the mounting structure (Figure 6).

E. coli K12 was the bacterium used throughout these experiments. Bacteria from stock culture on agar plates were inoculated into 500 ml of Trypticase Soy Broth (Sigma-Aldrich) and incubated in a shaker at 37 °C for approximately 18 hours until concentrations of 10^8-10^9 CFU/ml were achieved. The *p*H of the solution was approximately 7. The bacteria were then allowed to rest at room temperature for 1 hour before the suspension was poured into the radial horn cavity (Figure 6). Because ultrasonic vibrations can cause large increases in temperature in the fluid inside the horn, the horn was placed in a bath of iced water to maintain a low temperature throughout the test (<10 °C). This ensured that only inactivation due to sonication was observed and the contribution from thermal mechanisms was negligible. 0.5ml samples were removed aseptically from the horn at 30 second intervals over 5 minutes, serially diluted and plated on Trypticase Soy Agar (Sigma-Aldrich). Dilutions were made to 10^{-8} and 0.01 ml spots of each dilution were plated in triplicate. The plates were then incubated at 37 °C for 16 hours and the resulting colonies counted. Experiments were carried out in duplicate.

The two ultrasonic devices were operated at a power density of 12.57 W/cm^3, which represented the maximum available power to the probe device. A further test of the radial horn at a higher power density of 18.86 W/cm^3 was also conducted. During the experiments the probe device was placed in the same fluid volume as the radial horn and the probe was held at the centre of this volume at a depth such that foaming did not occur and the probe did not touch the bottom of the sonication cell.

Tests were also carried out at two different bacterial concentrations in order to observe if the bacterial inactivation rate was affected by initial bacterial concentrations. This was carried out for the radial horn only, at a power density of 12.57 W/cm^3. Two bacterial concentrations were used, one of approximately 2x10^9 CFU/ml and one of approximately 4x10^6 CFU/ml.

4. Results and Discussion

4.1 Comparison criteria

Table 1 shows the power input, intensity and power density associated with both the radial horn and probe device at the power levels used during this study. This table clearly shows that at similar power levels the probe horn has a much higher ultrasonic intensity (W/cm^2) due to the small area over which this power is distributed. The radial horn, having a much larger output surface area, has a much lower intensity. The power density (W/cm^3) of the two devices is easily matched because the same volume of liquid is being used throughout the tests and the power of both devices is similar.

4.2 Cavitation field visualisation

In order to visualise the cavitation field produced by the radial horn, digital images were taken using white backlighting and a Canon Ixus 50 digital camera. With tap water as the fluid, it was possible to capture pictures of the bubble clouds generated during ultrasonication. Figure 7 shows a clear bubble cloud in the centre of the fluid volume with streamers extending to the outer surface. This is expected, due to the focussing effect of the radial horn creating a low pressure area in the centre of the horn where cavitation can occur.

With a chemical method of visualisation, the sonochemiluminescence of both the radial and probe horns can be observed in Figure 8. The radial horn produces an intense SCL field close to the vibrating face at the lower *p*H (Figure 8(a)) whilst an intense luminescence field over the entire area is produced at the higher *p*H (Figure 8(c)). The probe device produces a cone shaped field of luminescence at *p*H 12 (Figure 8(d)), similar to that described by other researchers [11,24], but exhibits no luminescence at the lower *p*H 9.5 (Figure 8(c)). The cone shaped field can be more clearly seen in Figure 9 which is the same image as Figure 8(d) but with the colour levels adjusted.

It is proposed that the sonochemiluminescence observed for the radial horn at *p*H 9.5 is due to chemical reactions taking place involving the luminol solution and the aluminium horn. Kulmala et al. [26] have shown that chemiluminescence of luminol solutions can occur through reactions with aluminium. In their paper it was argued that the high *p*H of the solution breaks down the microscopic aluminium oxide layer which prevents any further oxidation of aluminium and thus allows the solution to come in contact with the aluminium metal and react chemically with it. It is also suggested that the breakdown of this layer is enhanced by the aspherical collapse of cavitation bubbles near a solid boundary which causes high speed jets to be formed and is known to cause erosion damage to surfaces. The results for the radial horn at the higher *p*H show an intense luminescence field throughout the fluid. This is caused by the luminol solution reacting with $OH^{\bullet}$ radicals produced

during bubble collapse. Although there is a cavitation focus in the centre, there are also streamers and bubble collapse is happening throughout the fluid which causes the entire volume to glow.

It can be seen that the cavitation fields of the radial and probe horns are quite different. The probe horn has its cavitation field in a cone shape in front of the tip and it has been shown that this area is also chemically active. The radial horn, however, focuses the cavitation field in the centre of the horn away from the vibrating face yet is very chemically reactive through the whole volume. Because the cavitation field is focussed in the centre of the horn, away from the working surface, significantly less cavitational damage to the device is observed as compared to probe devices which require titanium tips in order to maintain a good working life.

4.3 Bacterial inactivation results

Figure 10 shows the survival of *E. coli* K12 during treatments with the radial horn and probe horn for the same power density of 12.57 W/cm^3. It can be seen that the radial horn, operating at a lower ultrasonic amplitude than the probe device, produces improved bacterial inactivation. In fact, the radial horn provides an additional 0.3 log reduction in viable bacterial cells after exposure for 5 minutes. It is expected that this is as a result of the focussing of the cavitation field provided by the radial horn. It can also be observed that using the radial horn operating at a higher power density, of 18.86 W/cm^3, results in an additional 0.5 log reduction in bacterial numbers.

Although there have been studies into the effect of initial bacterial concentration on the inactivation kinetics using UV irradiation, heat, and pressure [27,28,29] there has been no published work to determine if initial concentration effects ultrasonic processes. The effect of the initial bacterial concentration on the inactivation efficiency of the radial horn can be seen in Figure 11. A greater bacterial inactivation is observed for the lower concentration of *E. coli* K12, with 99.9 % killing by approximately 3 minutes compared to 4 minutes for the higher concentration. In general, bacterial inactivation is regarded as an exponential process where the rate of inactivation is constant (first order kinetics) and does not vary with initial bacterial counts. This has been shown to be the case with UV radiation and heat [27,28]. However, other researchers [29,30] have found that the assumption of first order kinetics is not always valid. These results are consistent with the latter studies and it has been shown that the rate of inactivation is dependant on the initial bacterial count. This could be caused by a greater clumping of bacterial cells as the concentration increases, which provides some protection for the bacteria within the clump.

It is difficult to compare this work to previous studies in this field as all the studies concerning strains of *E. coli* have been carried out at significantly lower power levels. Studies by Allison (20 kHz, 60 W) [31], Hua (20 kHz, 80-140 W) [21], and Phull (20 kHz, 50 W) [32], investigated the ultrasonic treatment of *E. coli* suspensions. These studies showed that at the power levels used, the D-values, the time taken to reduce the bacterial concentration by one log count, ranged from 5 to over 30 minutes. In this study, for a probe device operating at 12.57 W/cm^3, representing a system operating at 20 kHz and 400 W, a 2 log reduction in viable cells was achieved within 5minutes, giving D-values of approximately 2.5 minutes. For the radial mode ultrasonic device operating at the same power density and frequency as the probe, a lower D-value of approx 2 minutes was achieved. Although this is still too long a time-scale to be incorporated into a flow-through device, it is possible that combining ultrasound with other bactericidal technologies, such as temperature, pressure and chlorine, could provide enhanced inactivation rates. The radial horn has been shown to be more effective than the probe device for inactivation of

E. coli K12 and has the additional advantage of being more adaptable to in-line flow-through processes.

5. Conclusions

This study has shown that a tuned radial horn operating at 20 kHz in the R0 mode has similar bacterial inactivation kinetics to a typical laboratory probe device vibrating in a longitudinal mode operating at the same power density. It has also been shown that the radial device can operate at a higher power density providing significantly better bacterial inactivation. Further, there is a concentration effect associated with ultrasonic processing and it takes longer to inactivate bacterial solutions with higher concentration levels of bacteria to the same percentage survival. There are a number of advantages to using the radial device for bacterial inactivation over the probe and these include the ease of adapting to continuous flow systems, lower cavitational damage to the device and a higher chemical activity spread through the volume of fluid.

6. References

1. Mason, T.J., Duckhouse, H., Joyce, E., Lorimer, J.P., WCU 2003, Paris, Sept 7-10, pp423-426, "Uses of ultrasound in the biological decontamination of water"
2. Mir, J., Morato, J., Ribas, F., Journal of applied microbiology, Vol.82, No.1, 1997, pp7-18, "Resistance to chlorine of freshwater bacterial strains"
3. Grant, I.R., Applied and environmental microbiology, Vol.62, No.2, 1996, pp631-636, "Inactivation of *mycobacterium paratuberculosis* in cows' milk at pasteurization temperatures"
4. Klijn, N. Herrewegh, A.A.P.M., De Jong, P., Journal of applied microbiology, Vol.91, 2001, pp697-704, "Heat inactivation data for *mycobacterium avium* subsp. p*aratuberculosis*: implications for interpretation"
5. Apfel, E., Holland C.K., Ultrasound in medicine and biology, Vol.17, No.2, 1991, pp197-185, "Gauging the likelihood of cavitation from short-pulse, low-duty cycle diagnostic ultrasound"
6. Suslick, K.S., In: Ultrasound. it's chemical, physical and biological effects, Chapter 4: homogeneous sonochemistry, VCH Publishers, 1988, pp125
7. Williams, P.R., Williams, R.L., Molecular physics, Vol.102, No.19-20, 2004, pp2091-2102, "Cavitation and the tensile strength of liquids under dynamic stressing"
8. Abramov, O.V., In: High intensity ultrasonics, Gordon and Breach Science Publishers, 1998
9. Leighton, T.J., In: The Acoustic Bubble, Academic Press, 1994, pp72-83
10. Piyasena, P., Mohareb, E., McKellar, R.C., International journal of food microbiology, Vol.87, 2003, pp207-216, "Inactivation of microbes using ultrasound: a review"
11. Sala, F.J., Burgos, J., Condon, S., Lopez, P. ,Raso, J., In: New methods of food preservation, Chapter 9, Springer, 1995, pp186
12. Villamiel, M., De Jong, P., Journal of food engineering, Vol.45, 2000, pp171-179, "Inactivation of *pseudomonas fluorescens* and *streptococcus thermophilus* in trypticase soy broth in milk by continuous-flow ultrasonic treatment and conventional heating"
13. Garcia, M.L., Burgos, J., Sanz, B., Ordonez, J.A., Journal of applied bacteriology, Vol.67, 1989, pp619-628, "Effect of heat and ultrasonic waves on the survival of two strains of *bacullus subtilis*"

14. Zenker, M., Heinz, V., Knorr, D., Journal of food protection, Vol.66, No.9, 2003, pp1642-1649, "Application of ultrasound-assisted thermal processing for preservation and quality retention of liquid foods"
15. Grundy, M.A., Bolek, W.E., Coakley, W.T., Benes, E., Journal of immunological methods, Vol.165, 1993, pp47-57, "Rapid agglutination testing in an ultrasonic standing wave"
16. Lucas, M., Ultrasonics, Vol.34, No.1, 1996, pp35-41, "Vibration sensitivity in the design of ultrasonic forming dies"
17. O'Shea, K., ASME Design Engineering Division DE, Vibration Analysis - Analytical and Computational, Vol.DE-37, 1991, pp259-265, "Enhanced vibration control of ultrasonic tooling using finite element analysis"
18. Ewins, D.J., In: Modal testing theory practice and application, 2nd Edition, Research studies press ltd., 2000
19. Duckhouse H., Mason, T.J., Phull, S.S., Lorimer, J.P., Ultrasonics sonochemistry, Vol.11, 2004, pp173-176, "The effect of sonication on microbial disinfection using hypochlorite"
20. Blume, T., Neis, U., Ultrasonics sonochemistry, Vol.11, 2004, pp333-336, "Improved wastewater disinfection by ultrasonic pre-treatment"
21. Hua, I., Thompson, J.E., Water research, Vol.34, No.15, 2000, pp3888-3893, "Inactivation of *escherichia coli* by sonication at discrete ultrasonic frequencies"
22. De Gennaro, L., Cavella, S., Romano, R., Masi, P., Journal of food engineering, Vol.39, 1999, pp401-407, "The use of ultrasound in food technology I: inactivation of peroxidase by thermosonication"
23. McMurray, H. N., Wilson, B. P., Journal of physical chemistry A, Vol.103, 1999, pp3955-3962, "Mechanistic and spatial study of ultrasonically induced luminol chemiluminescens"
24. Moussatov, A., Granger, C., Dubus, B., Ultrasonics sonochemistry, Vol.10, 2003, pp191-195, "Cone-like bubble formation in ultrasonic cavitation field"
25. Joyce, E., Phull, S.S., Lorimer, J.P., Mason, T.J., Ultrasonics sonochemistry, Vol.10, 2003, pp.315-318, "The development and evaluation of ultrasound for the treatment of bacterial suspensions. A study of frequency, power and sonication time on cultured *bacillus* species"
26. Kulmala, S., Matachescu, C., Kulmala, A., Papkovsky, D., Hakansson, M., Ketama, H., Canty, P., Analytica chimica acta, Vol.453, 2002, pp253-267, "Chemiluminescence of luminol induced by dissolution of oxide-covered aluminium in alkaline aqueous solution"
27. Watts, R.J., Kong, S., Orr, M.P., Miller, G.C., Henry, B.E., Water research, Vol.29, No.1, 1995, pp95-100, "Photocatalytic inactivation of coliform bacteria and viruses in secondary effluent"
28. Sung, N., Collins, M.T., Applied and environmental microbiology, Vol.63, No.3, 1998, pp999-1005, "Thermal tolerance of *mycobacterium paratuberculosis*"
29. Furukawa, S., Noma, S., Shimoda, M., Hayakawa, I., International journal of food science and technology, Vol.37, 2002, pp573-577, "Effect of initial concentration of bacterial suspensions on their inactivation by high hydrostatic pressure"
30. Chiruta, K., Davey, K.R., Thomas, C.J., Transactions of the institute of chemical engineers: food and bioproducts processing, Vol.75, No.3, 1997, pp174-180, "Thermal inactivation kinetics of three vegetative bacteria as influenced by combined temperature and *p*H in a liquid medium"
31. Allison, D.G., D'Emanuele, A., Eginton, P., Williams, Journal of basic microbiology, Vol.36, No.1, 1996, pp3-11, "The effect of ultrasound on *escherichia coli* viability"

32. Phull, S.S., Newman, A.P., Lorimer, J.P., Pollet, B., Mason, T.J., Ultrasonics sonochemistry, Vol.4, 1997, pp157-164, “The development and evaluation of ultrasound in the biocidal treatment of water”

Horn	Power (W)	Intensity (W/cm^2)	Power Density (W/cm^3)
Radial	400	9.43	12.57
Radial	600	14.15	18.86
Probe	400	301.35	12.57

Table 1 Summary of intensities and power densities for radial and probe horns

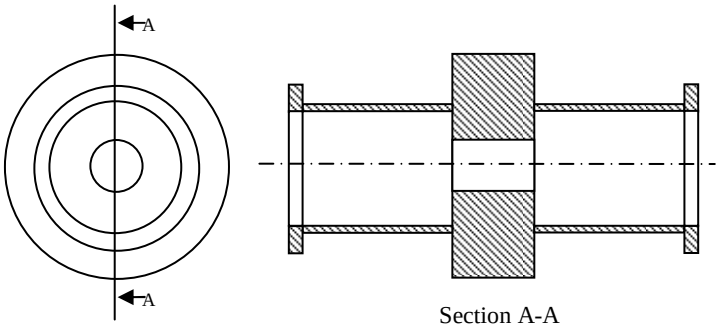

Figure 1 Ultrasonic radial horn

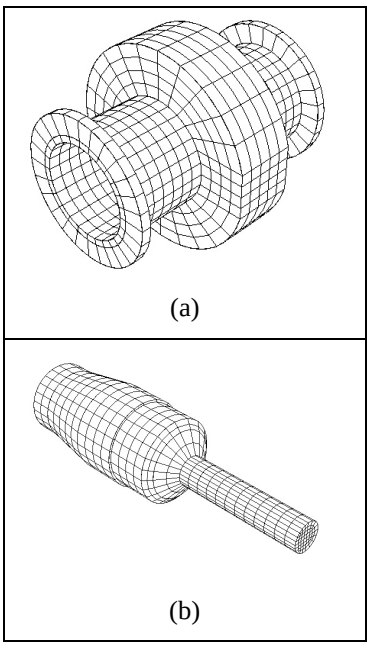

(a)

(b)

Figure 2 FEA mesh of (a) radial horn, (b) probe horn.

FEA	EMA
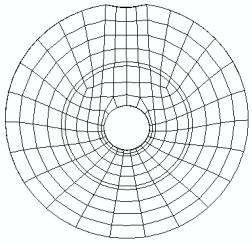 R1 mode at 18086 Hz	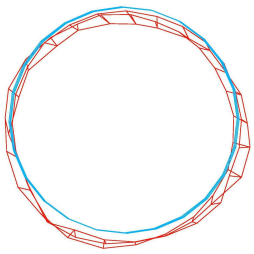 R1 mode at 18173Hz
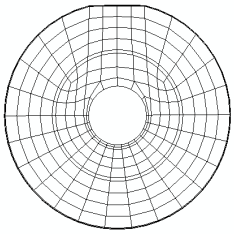 R0 mode at 19880 Hz	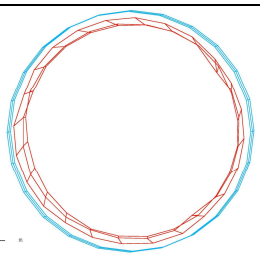 R0 mode at 19980Hz
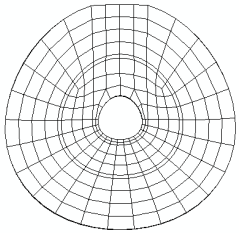 R3 mode at 22144 Hz	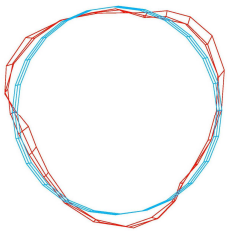 R3 mode at 22060Hz

Figure 3 Comparison of radial horn modal frequencies and mode shapes from FEA and EMA

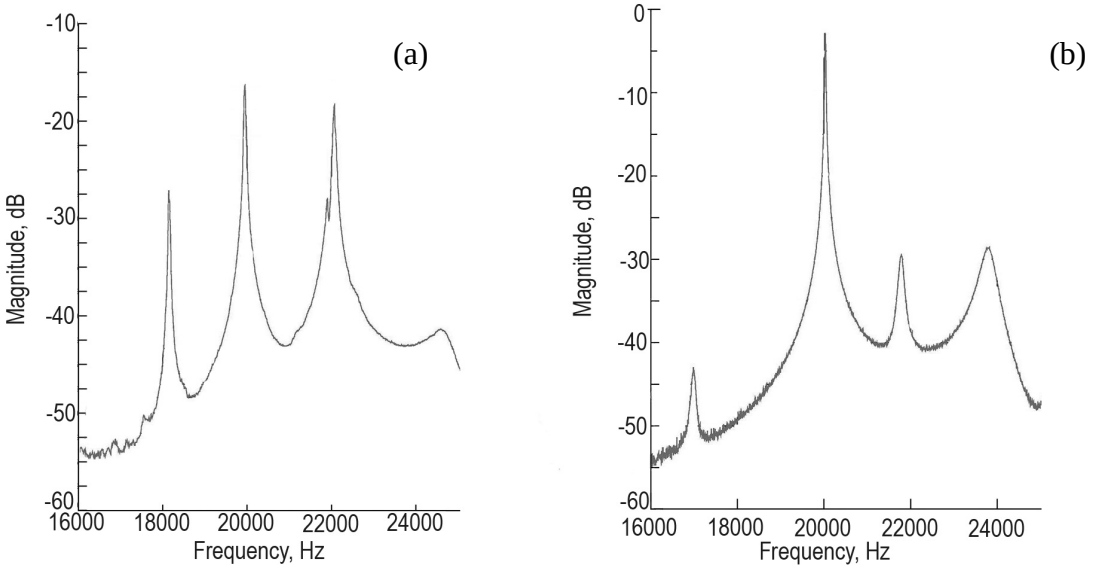

Figure 4 FRF of (a) radial horn and (b) probe horn, between 16 kHz and 25 kHz.

FEA	EMA
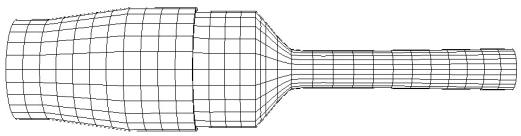	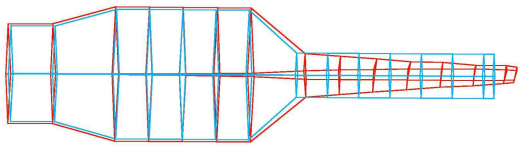
Longitudinal mode at 20030 Hz	Longitudinal mode at 20026 Hz
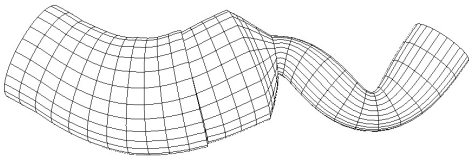	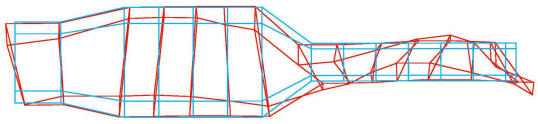
3rd bending mode at 21442 Hz	3rd bending mode at 21794 Hz
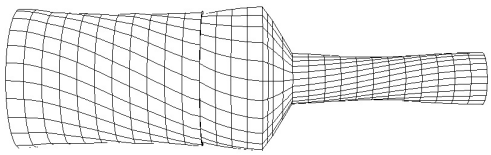	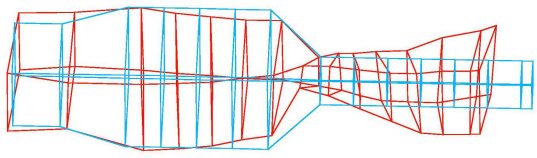
2nd torsional mode at 23825 Hz	2nd torsional mode at 23804 Hz

Figure 5 Comparison of probe horn modal frequencies and mode shapes from FEA and EMA

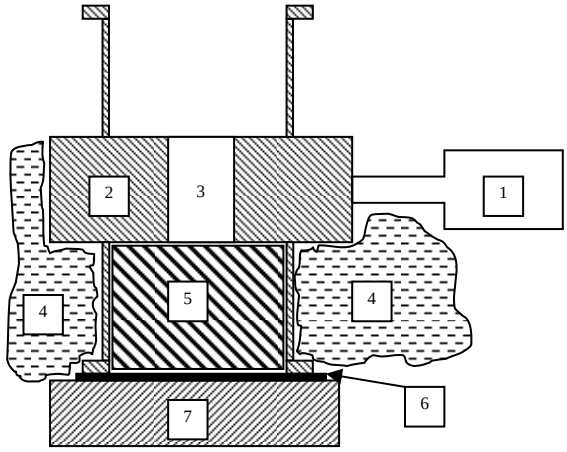

Figure 6 Experimental set-up showing (1) 20 kHz ultrasonic transducer, (2) radial horn, (3) volume of fluid containing bacteria, (4) ice packing, (5) plastic insert, (6) rubber gasket, (7) aluminium mounting flange

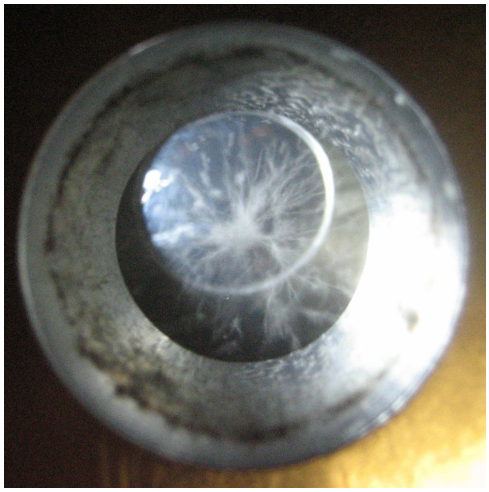

Figure 7 Photograph of cavitation field using backlighting

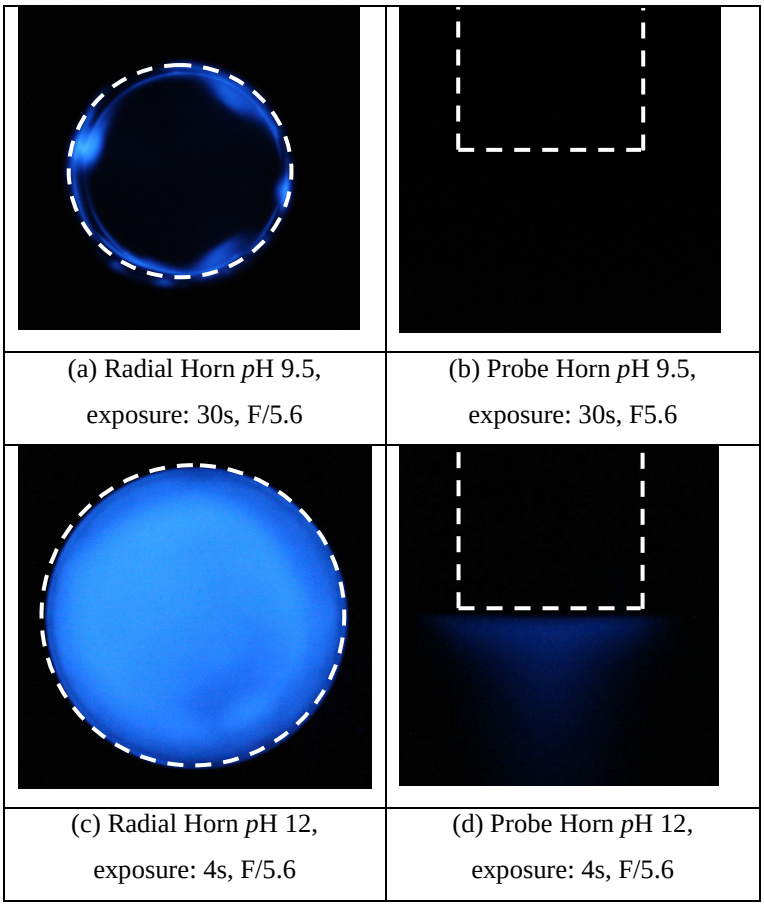

(a) Radial Horn *p*H 9.5, exposure: 30s, F/5.6

(b) Probe Horn *p*H 9.5, exposure: 30s, F5.6

(c) Radial Horn *p*H 12, exposure: 4s, F/5.6

(d) Probe Horn *p*H 12, exposure: 4s, F/5.6

Figure 8 Photographs of sonochemiluminescence; (a) radial horn *p*H 9.5, (b) probe horn *p*H 9.5, (c) radial horn *p*H 12, and (d) probe horn *p*H 12.

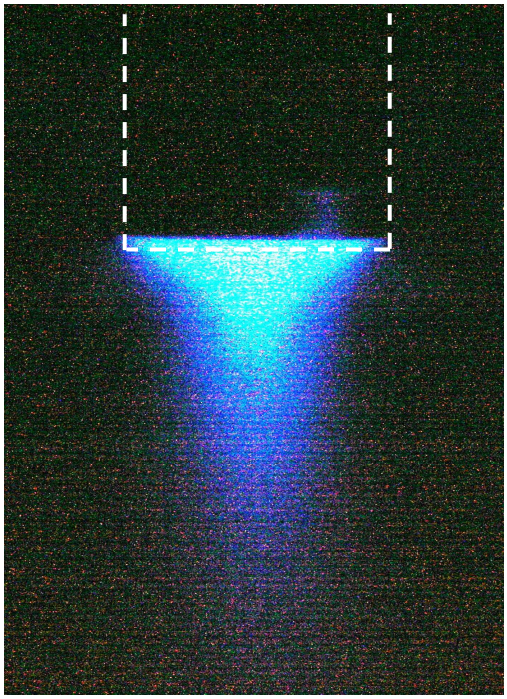

Figure 9 Probe luminescence field at *p*H 12, colour levels adjusted

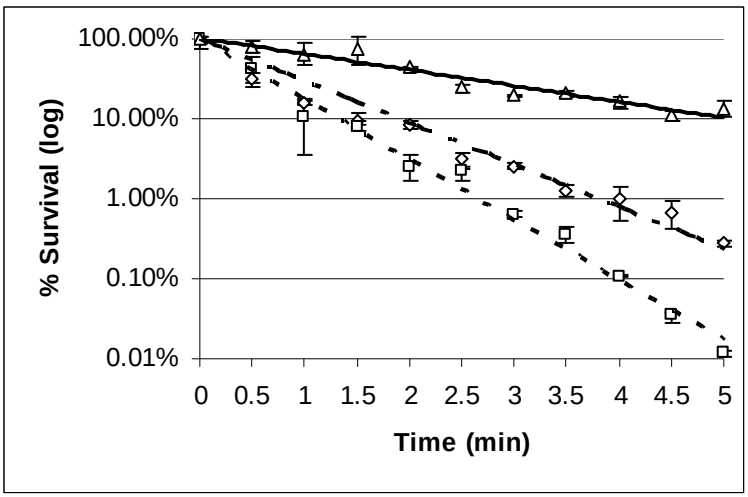

Figure 10 Bacterial inactivation as a function of exposure time for: □ radial horn 18.86 W/cm^3, ◊ radial horn 12.57 W/cm^3, Δ probe horn 12.57 W/cm^3

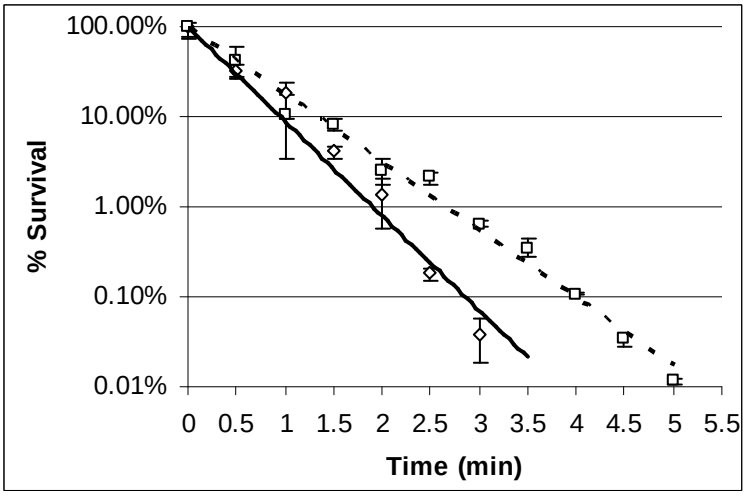

Figure 11 Effect of concentration on % survival, □ 2x10^9 CFU/ml, ◊ 4x10^6 CFU/ml